NJC

Synthesis, crystal structure, optical and electrochemical properties of novel diphenylether-based formazan derivatives

Journal:	*New Journal of Chemistry*
Manuscript ID:	NJ-ART-12-2014-002353.R1
Article Type:	Paper
Date Submitted by the Author:	16-Jan-2015
Complete List of Authors:	Berber, Halil; Anadolu University, Department of Chemistry Türkoğlu, Gülşen; Anadolu University, Department of Chemistry Kani, İbrahim; Anadolu University, Department of Chemistry

Journal Name

RSCPublishing

ARTICLE

Synthesis, crystal structure, optical and electrochemical properties of novel diphenylether-based formazan derivatives

Cite this: DOI: 10.1039/xoxxoooooox

Received ooth January 2012,
Accepted ooth January 2012

DOI: 10.1039/xoxxoooooox

www.rsc.org/

Gulsen Turkoglu,[a] Halil Berber[a]* and Ibrahim Kani[a]

In this study, formazans **5a**−**5h** were synthesized by coupling reactions of substituted phenylhydrazone compounds **3a**−**3h** with diazonium salt of 4-chloro-2-phenoxybenzenamine (**4**). The substituted phenylhydrazones **3a**−**3h** were obtained from the condensation of substituted phenylhydrazines **1a**−**1h** with 4-methoxybenzaldehyde (**2**). The structures of the formazans were characterized by using elemental analysis, FTIR, ^{1}H NMR, ^{13}C NMR, LC-MS and the crystal structure of compound **5e** was determined by X-ray crystallography. Absorption spectra of all compounds were investigated in different solvents. Although their absorption bands are very little dependent on the polarities of solvents, the significant change was observed with altering the electronic character of the substituents. The fluorescence quantum yield properties and Stokes shifts of compounds **5a**−**5h** in DMSO were also explored. Electrochemical properties of the new products were studied by CV measurements. In addition, computational studies were conducted at PBE1PBE/6-311g (2d,2p) level to shed light on the structures of possible tautomers and intramolecular H-bonds.

Introduction

Formazans were first synthesized over a century ago, but still attract attention of chemists, biologists, technologists and other specialists.[1] Numerous studies have been devoted, such as their syntheses, structural and spectroscopic properties,[2-5] photochemical transformations,[6,7] tautomer formation,[8,9] and synthesis of crown formazans[10] and broad spectrum of biological activities.[11-15] In addition, formazan derivatives were reported to be used for the synthesis, optical properties, electrochemical behaviours of metal[16-20] and boron complexes as functional materials.[21-23]

Formazans form tetrazolium salt when they are oxidized. The tetrazolium/formazan couple is a special redox system acting as proton acceptor or oxidant; this system is now widely applied in different branches of the biological science for example, medicine, pharmacology, immunology, and botany, but especially in biochemistry and histochemistry.[24,25] These features cause an increasing interest especially in electrochemical and spectral properties of tetrazolium/formazan systems.[26,27] As a predictive tool for electronic structural properties, molecular modelization techniques allow a solution for the interpretation of experimental data. For the calculation of electronic structures of large molecules, the most widely used method is density functional theory (DFT).[26,28] Tautomerism, which is extremely important in the structure and properties of formazans, and intramolecular hydrogen bridge in some formazans were studied by means of DFT.[28,29]

Diphenylether derivatives find applications in many areas. They have been used as biocides, flame retardants, functional fluids and motifs in many natural products. Among biocides they have been used as herbicides, antibacterial, antitubercular properties, and also copolymers.[30-32] Formazans containing diphenylether are anticipated to be intriguing organic compounds in medicinal and material applications.

In our previous work, a new formazan derivative was synthesized and used for the modification of pencil graphite electrode for determination of paracetamol in electrochemical sensor applications.[33] Herein, we synthesized new eight compounds **5a**−**5h** by coupling reactions of phenylhydrazones (**3a**−**3h**) with appropriate diphenylether substituted aryldiazonium chlorides in pyridine

(Scheme 1) in order to shed light on the physical and chemical properties of formazan derivatives. The structures of all synthesized molecules were characterized using elemental analysis, various spectroscopic methods and the structure of representative compound **5e** was unambiguously confirmed based on the X-ray crystallography. The absorptions of the compounds were investigated in solvents with different polarities. The dependence of their absorption spectra on the substituents was studied. The fluorescence quantum yield properties and Stokes shifts of compounds **5a**−**5h** in DMSO were explored. Electrochemical properties of the new products were investigated by cyclic voltammetry. In addition, the results of the calculations at PBE1PBE/6-311g (2d,2p) level were taken into the consideration to determine the possible tautomer structures and intramolecular hydrogen bond of all synthesized compounds.

Results and discussion

Synthesis

The substituted phenylhydrazones used as the initial substances were obtained via condensation reactions of substituted phenylhydrazines with 4-metoxybenzaldehyde resulting in good to excellent yields (75−98%). **3a**−**3h** were characterized using FTIR, ^{1}H NMR, ^{13}C NMR and elemental analysis (see ESI†).

In this work, formazans **5a**−**5h** were synthesized according to the first method reported by Nineham[34] namely the coupling of substituted phenylhydrazones with 4-chloro-2-phenoxybenzenamine diazonium cation in a basic media at 0 ºC (Scheme 1).

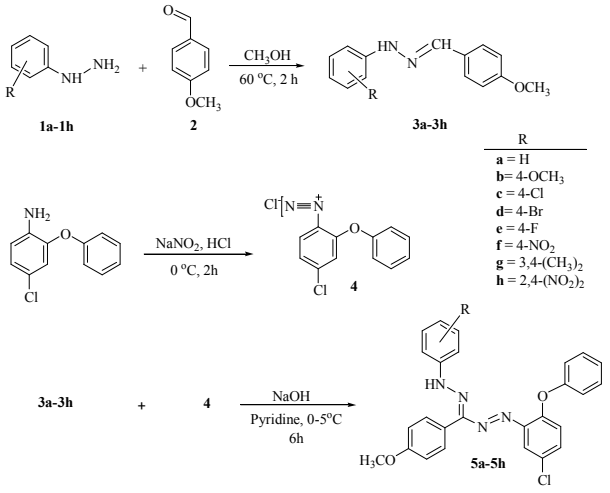

Scheme 1 Synthetic route for the formation of formazan derivatives **5a**−**5h**.

Although pyridine was a characteristic of a strong catalyst which abstracts proton[34] improvement of the reaction condition was achieved by addition of a solution of NaOH with pyridine, because the coupling step was also largely governed by pH of the medium. The optimum level was found to be pH ≥ 12, while at pH ≤ 9 the product formed a sticky material that clung to the stirring bar, leaving the reaction incomplete. Moreover, the position and steric effects of the substituents located at the phenyl group of benzaldehyde unit of the starting material affect the coupling reactions significantly. Therefore, *para*-substituted phenyl was chosen to avoid the steric effects. Synthesized compounds were purified by recrystallization from methanol. While a coupling reaction of diazonium salt with **3a** possessing unsubstituted phenyl group gave a corresponding product **5a** in 82% yield, halogenated ones (Cl, Br and F) resulted in good to excellent yields (70−86%). The other compounds **5b** and **5f**−**5h** gave rise to moderate yields (49−62%). Analytical and spectral data supported fully the structure of all compounds.

Characterizations

The FTIR spectra of all synthesized formazans **5a**−**5h** were recorded using the solid KBr pellets technique in the 400−4000 cm^{-1} range. The characteristic IR frequency bands are given in Experimental section. Absence of N−H absorption bands between 3100 and 3500 cm^{-1} verify the six-membered pseudo aromatic ring with intramolecular hydrogen bond Ph^{1}−NH ··· N−Ph^{5} in formazan skeleton.[35,36] Observation of weak bands in the range of 3055−3093 cm^{-1} for all compounds indicated the existing of intramolecular hydrogen bond in formazans. The sharp characteristic −C=N− tension vibration bands were observed between 1589−1610 cm^{-1} pointing out the existence of intramolecular hydrogen bond (Scheme 2).[37,38] The observation of intense bands between 1461−1496 cm^{-1} demonstrated the −N=N− group, which was well in agreement with the reported FTIR values.[2,4]

^{1}H NMR spectrum data and the calculated coupling constants for **5a**−**5h** were given in experimental section. The downfield −NH peak of formazans was characteristic and indicated the presence of an intramolecular hydrogen bond.[39] Due to the existence of hydrogen bonds inside the molecule, NH proton is detected as a singlet in the downfield **5a**−**5g** between 14.87−15.38 ppm.[9,10] However, weakening of the intramolecular hydrogen bonds, emerged most probably from the electronic effect of the attached NO_2 group, points out the upfield shift of −NH proton (**5h**, 13.95 ppm).[13,17,40] The observation of these values confirm the presence of pseudo aromatic

−NH−N molecular hydrogen bond in formazan skeleton (−NH−N=C−N=N−) (Scheme 2). The chemical shifts of the aromatic protons were recorded between 8.88 and 6.83 ppm as expected. While methoxy protons (−OCH_3) were observed as a singlet between 3.86−3.80 ppm, methyl groups (−CH_3) in the compound **5g** detected in the upfield (2.20 − 2.30 ppm).

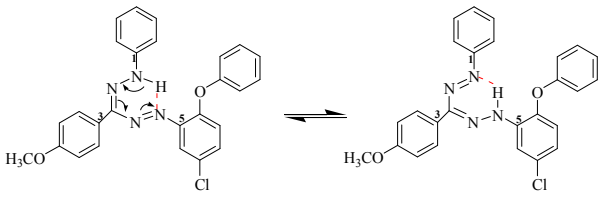

Scheme 2 Intramolecular hydrogen bonding and tautomerisation of the formazan system.

^{13}C NMR spectra of formazans **5a**−**5h** were given in experimental section. The obtained peaks belonging to carbon atoms in −N−C=N− units of **5a**−**5h** were recorded in downfield between 165.37 and 159.69 ppm, which are well in agreement with reported literature values.[38,41] While aliphatic −OCH_3 carbon atoms observed in the range of 55.42 − 55.37 ppm, methyl groups attached to **5g** were appeared at 19.92 − 19.67 ppm. ^1H NMR and ^{13}C NMR spectra confirmed the validity of the structures given in Scheme 1.

The mass spectra data of the formazans **5a**−**5h** were given in Experimental section. While in the mass spectrum of the compound **5a** ($C_{26}H_{21}ClN_4O_2$, M = 456.92 g/mol) the molecular ion peak was observed to be MS $(ESI)^+$: *m/z* = 456.1 (18%, M^+) , fragmentation of 1-position phenyl and 5-position unsubstituted phenyl radical cations led to the residual molecule having a mass of 304.3 (87%, M-$C_{14}H_{11}N_4ClO_2^+$). All synthesized compounds were evaluated in the same manner and the results obtained from the mass spectra confirmed the validity of the structures given in Scheme 1.

Crystal structure

The molecular view of **5e** is shown in Fig. 1 and some selected bond lengths and angles are given in Table S1. **5e** (red needles) crystallizes in orthorhombic system with Z = 8 in space group Pbca. All bond lengths and angles were within the normal ranges. X-ray investigation of the compound **5e** showed that tautomer 2 structure was favoured in the solid state (see Fig. 1). The molecule of **5e** has –C=N– and –N=N– double bond [C8–N1=1.307(3), N3–N4=1.277(3) Å]. The exocyclic C–C–N bond angles around the C15 atom are asymmetrical. The C16–C15–N4 angle (114.1(2)°) is significantly smaller than the C20−C15−N4 angle (125.7(2)°). C8–N3–N4 (114.8(2)°) and C8–N1–N2 (120.1(2)°) angles around the N1, N3 atoms are not equal to each other. The aromatic rings in the molecule have usual bond lengths and angles. The **5e** has a strong intramolecular N2–H2···N4 hydrogen bond with D–H, D···A and H···A distances of 0.89(3), 2.549 (3) and 1.87(3) Å, respectively, and D – H···A angle of 132.3 (3)° as shown Fig. 1.

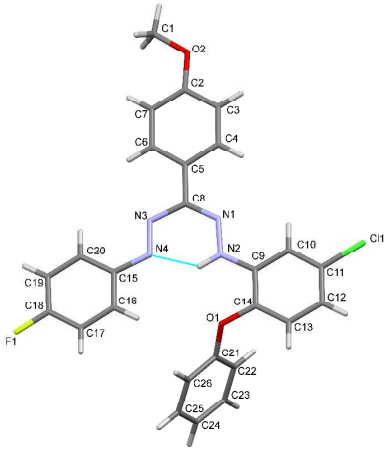

Fig. 1 Molecular structure of compound **5e**.

This bond indicated the formation of a six-membered pseudo aromatic ring in the molecule due to the inner-molecular hydrogen transfer, which is also responsible for its tautomers. The molecule has almost planar conformation. The torsion angle is 4.3 (4)° for N3–N4–C15–C20 and -3.1 (4)° N1–N2–C9–C10. In the asymmetric unit of the molecule, the dihedral angle between the least square planes of the phenyl rings R1 [C2–C3–C4–C5–C6–C7], R2 [C9–C10–C11–C12–C13–C14], R3 [C15–C16–C17–C18–C19–C20], R4 [C21–C22–C23–C24–C25–C26] and the pseudo six-membered aromatic ring R5 [C8–N1–N2–N3–N4–H2] are given in Table 1 (see Fig. 2 (a)).

Table 1 Dihedral angles between the least-squares planes of rings

Ring No	Ring No	Dihedral Angle (°)
R1	R2	7.38 (1)
R1	R3	8.81 (1)
R1	R4	72.46 (2)
R1	R5	5.47 (1)
R2	R3	3.41 (1)

R2	R4	62.94 (2)	R4	R5	74.08 (2)
R2	R5	2.96 (1)			
R3	R4	77.04 (2)			
R3	R5	6.05 (1)			

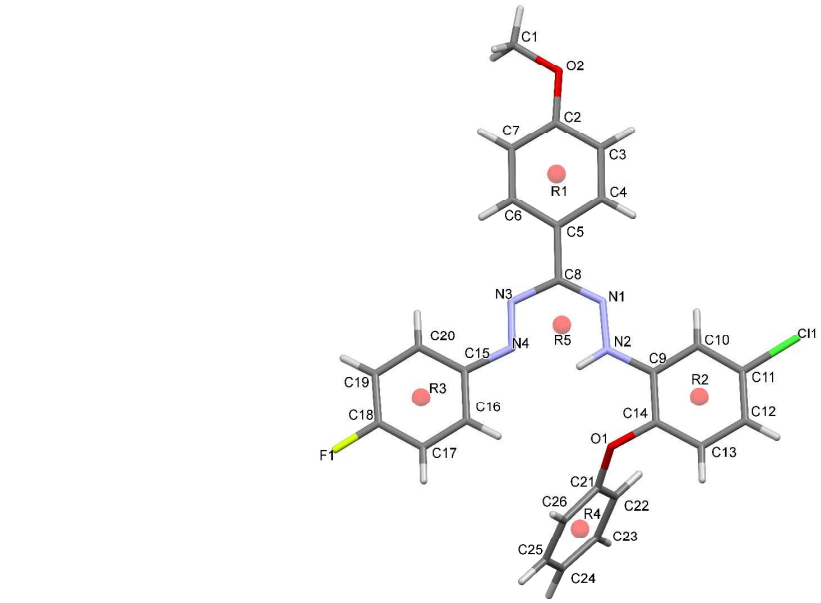

a)

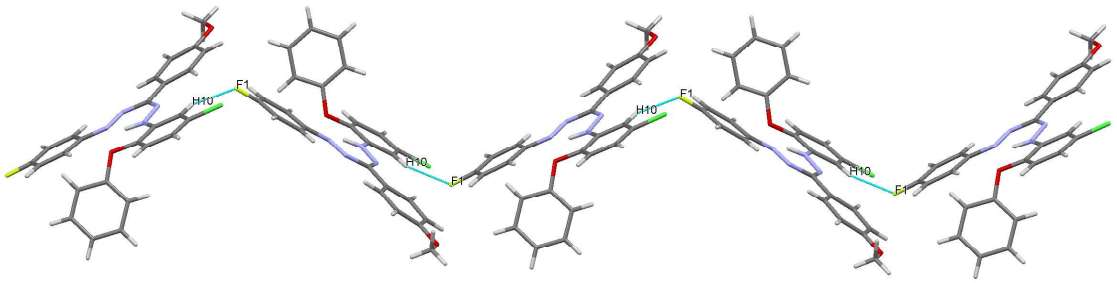

b)

Fig. 2 a) View of the center of rings in **5e**. b) Chain formation in the crystal structure along the b-axis through hydrogen bond.

The shortest intermolecular π-ring distance of 4.035 Å is observed between R2 and R3. Moreover, there exist weak intermolecular interactions between C4–F1^{i}, C10-F1^{i}, C25–O2^{ii} and C1–O2^{iii}. The distances are 3.609(3), 3.260(3), 3.732(3) and 3.580(4) Å, respectively (symmetry codes i : -x+1/2+1,-y+2, +z+1/2, ii : -x+1/2+1,-y+2, +z-1/2, iii : x+1/2, +y,-z+1/2). The molecules in the crystal structure are stacked along the b-axis through hydrogen bond of C10–F1 as shown Fig. 2 (b).

Absorption spectra

The UV-Vis. studies of the synthesized formazans **5a**–**5h** were carried out in solvents with fourteen different polarities and the results are listed in Table S2 (see ESI†). The stock solutions of the compounds were prepared in a 1×10^{-5} mol L^{-1} concentration. The

UV-Vis. spectra of compound **5a** within different solvents are given in Fig. 3. The observed visible band in formazans was a result of π–π* transition of the *N*,*N*–diarylhydrazone conjugated system.[42,43] Since the formazan skeleton has a structure showing the tautomerization, the characteristic bands belong to the π–π* transitions (Fig. 3).[1]

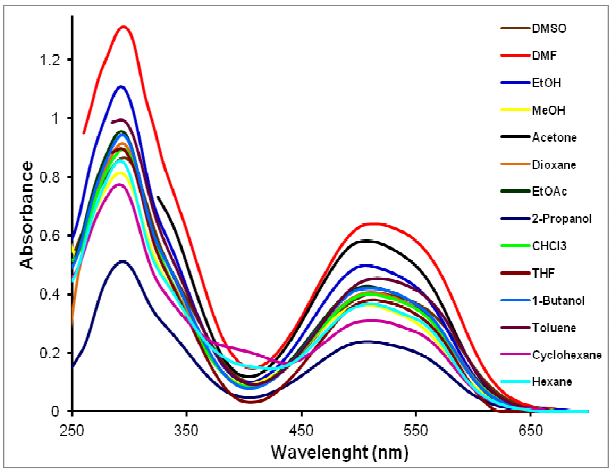

Fig. 3 Electronic absorption bands of compound **5a** in various solvents.

The compounds **5a**–**5g**, in accordance to the figures in the literature, produced wide bands between λ_{max1} of 494 − 554 nm in different polarity solvents, which belong to the characteristic π–π* transitions in the formazan skeleton and demonstrated the existence of a six-membered ring in formazan skeleton due to the inner-molecular hydrogen transfer (Scheme 2).[44] Contrary to the other compounds, **5h** (λ_{max1} = 366–400 nm**)** showed the blue shift in solvents due to the fact that it forms the equilibrium structure possessing hydrogen bond between oxygen of *orto*-NO_2 group with Ph^1–NH and consequently suppressed the formation of hydrogen bond in the formazan skeleton (Scheme 3).[45,46]

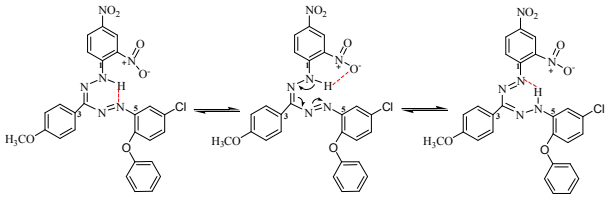

Scheme 3 The formation of hydrogen bond between the –NO_2 and N–H and NH···N=N groups in compound **5h** (red dash line=H-bond).

The second band λ_{max2} appearing in the range of 294 − 335 nm emerged from π–π* transitions within the hydrogen bond formed by the azo and hydrazo groups and the tautomerization in Scheme 2.[36] In accordance to the literature values, for the compounds **5a**–**5e**, **5g** the inner-molecular hydrogen bonds were seen in the λ_{max2} of 294 − 303 nm belonging to the π–π* electronic transitions of the chelate rings. Formazan **5f** demonstrated this band in between 358 − 393 nm which might arise from an intramolecular charge transfer from solute–solvent interaction in the form of hydrogen bonding or bulk solvent properties. These values in the absorption spectra of formazan derivatives have supported the presence of an intramolecular hydrogen transfer over formazan skeleton.

Effect of solvent on the absorption spectra. Effects of solvent polarity on absorption of these formazans were summarized in Table S2. Absorption properties of the formazans have shown some dependence on the polarity of the solvents (Fig. 3). With increasing polarity of the solvents, the absorption peak position of formazans **5a**–**5d** and **5g** exhibited generally a red shift up to 28 nm, in addition to, that of **5h** depicted obvious red shift between 10 and 34 nm. This can be mainly attributed to the fact that solvation by a polar solvents stabilizes π and π* orbitals.[36] Consequently, the decrease of π–π* transition energy concerning intramolecular charge transfer (ICT) band within whole molecule was observed.[47] Compound **5e** demonstrated a bathochromic shift of 4 to 10 nm in non-polar solvents, such as toluene, cyclohexane and *n*-hexane. With increasing the polarity of solvents, the absorption peak of compound **5f** (λ_{max} = 24 − 79 nm) was shifted to shorter wavelength, thus exhibiting a negative solvatochromism, because the ground state was more stabilized in a solvent cage of already partly oriented solvent molecules with stronger polarity. While compounds **5a**–**5d** and **5g**–**5h** showed slight positive solvatochromism, compounds **5e** and **5f** demonstrated negative solvatochromism in polar solvents. The longest wavelength maximum was found at 554 nm in toluene, whereas the highest hypsochromic shift was observed at 366 nm in cyclohexane. These changes were attributed to the hydrogen–bonding interaction between the solute and solvent molecules or intramolecular charge transfer within the whole molecule.

Substituent effect on the absorption spectra. The substituent effects on characteristic λ_{max1} values of formazans **5a**–**5h** were examined in methanol, THF and toluene (Table 2). The peak shift values ($\Delta\lambda_{max}$) were determined according to the difference between the λ_{max1} value of parent compound **5a** and λ_{max1} values of

substituted formazans **5b**–**5h**.[45,46] The UV-Vis spectra of all the compounds are given in toluene (Fig. 4).

Table 2 UV-Vis spectra of compounds **5a**–**5h** λ_{max1} (nm) and peak shift ($\Delta\lambda_{max}$) values, (1×10^{-5} M).

		Methanol		THF		Toluene	
Comp	Substituent	λ_{max} nm	$\Delta\lambda_{max}$ [a]	λ_{max} nm	$\Delta\lambda_{max}$ [a]	λ_{max} nm	$\Delta\lambda_{max}$ [a]
5a	4-H	506	-	509	-	515	-
5b	4-OCH_3	493	13	505	4	518	-3
5c	4-Cl	525	-19	534	-25	538	-23
5d	4-Br	521	-15	530	-21	535	-20
5e	4-F	504	2	511	-2	522	-7
5f	4-NO_2	546	-40	537	-28	554	-39
5g	3,4-$(CH_3)_2$	501	5	508	1	516	-1
5h	2,4-$(NO_2)_2$	390	116	380	129	378	137

[a] $\Delta\lambda_{max} = \lambda_{max1}$ (unsubstituted formazan (**5a**)) – λ_{max1} (substituted formazan (**5b**-**5h**)).

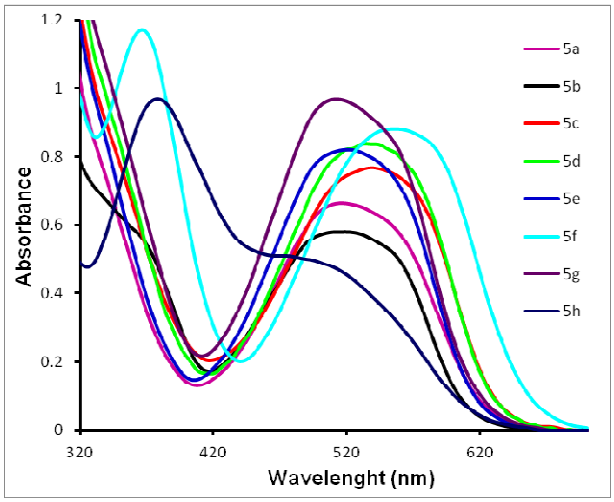

Fig. 4 Electronic absorption bands of all compounds in toluene.

As seen in methanol in Table 2, the absorption value (λ_{max1}) of compound **5b** possessing electron donating –OCH_3 subunit at *para* position was recorded 13 nm lower than the parent molecule in methanol. In both –Cl and –Br substituted compounds **5c** and **5d**, the λ_{max1} values pronounced bathochromic shifts of 19 nm and 15 nm, respectively. Under these circumstances, the –Cl and –Br atoms, acting as an inductive electron withdrawing and a resonance electron donating effects, ended up with two opposite effects. It can be seen that they acted as weak electron withdrawing groups. The high electronegativity of fluorine group attached to the 1-phenyl ring resulted in smallest bathochromic shifts in THF and toluene (for compound **5e** $\Delta\lambda_{max}$ = 2−7 nm relative to compound **5a** in methanol). The λ_{max1} value of the compound **5f**, which included the *para*–NO_2 group on 1-phenyl ring with its strong electron withdrawing effect, showed bathochromic shifts ($\Delta\lambda_{max}$ = 28−40 nm), compared to **5a**. λ_{max1} value of the compound **5g** substituted by –CH_3 group, which is inductive as electron donating at *meta*- and *para*-positions, showed little hypsochromic shift ($\Delta\lambda_{max}$ = 1−5 nm). The fact that λ_{max1} value of the compound **5h** substituted with a strong electron attractive –NO_2 group at positions *ortho*- and *para*- in 1-phenyl ring introduced shift towards lower wavelength ($\Delta\lambda_{max}$ = 116 nm) compared to **5a**. This phenomenon can only be explained by the formation of a possible hydrogen bond between N−H proton with oxygen of a –NO_2 group attached to the *orto*-position of the 1-phenyl ring (Scheme 3).[45,46] Therefore, the electron attractive quality of the *ortho*–NO_2 group decreases progressively and the resonance effect disappears.[45,46] According to these results, generally electron donating groups lead to hypsochromic shifts, whereas the electron withdrawing units resulted in bathochromic shifts.

Fluorescence Spectra

Fluorescence spectra of the target materials under excitation at 470 nm are depicted in Fig. 5b. Exciting at the λ_{max} of most formazans showed either no fluorescence or fluorescence of very low intensity suggesting that fluorescence does not come from the species responsible for λ_{max} absorption. Fluorescence was measured at low concentrations to avoid aggregation, self-absorption effects, excimers, and emission spectrum distortion.[48,49] The 470 nm excitation wavelength provided the highest fluorescence level, and was a useful wavelength for quantum yield comparison.

Compounds (**5a**–**5h**) afforded a green to yellow emission with the maxima varying from 510 to 570 nm in DMSO (Table 3). Compound **5a** exhibited a yellow fluorescence with the emission maximum of 570 nm, which is the highest among the other compounds (Fig. 5b). Due to strong electron-withdrawing ability of NO_2 group on the 1-phenyl ring, compound **5f** and **5h** were blue-shifted by 57 and 110 nm, respectively, compared to **5a**. These were consistent with results recorded from the UV-vis absorption spectra of these compounds. Compound **5g**, which has 3,4-dimethyl group

on the 1-phenyl ring, also exhibited green fluorescence with maximum at 561 nm. The emission maximum of **5b**, having a methoxy substitution on the 1-phenyl ring, was blue-shifted by 4 nm, compared to **5a**. Compared with that of compound **5c** (λ_{em} = 556 nm), the emission maxima of compound **5d** (λ_{em} = 553 nm) and compound **5e** (λ_{em} = 564 nm) were red shifted about 8 and 11 nm, respectively. The difference of electron withdrawing and donating capability of substituents on the 1-phenyl ring, and the difference in the degree of conjugation caused the above phenomenon.

The Stokes shifts of compounds **5a**–**5h** were calculated from the difference between λ_{em} and the excitation wavelength of 470 nm (Table 3). Stokes shifts of formazans were also dependent on the groups bonded to 1-phenyl ring. While compound **5a** with no substitute on the 1-phenyl ring exhibited a large Stokes shift of 100 nm, those of the other compounds were obtained between 40 and 96 nm. The Stokes shifts detected in the emission spectra were attributed to electronic transitions and an intramolecular charge transfer (ICT) from Ph^1–NH donor to the N–Ph^5 acceptor (Scheme 2). The intramolecular CT resulted in increment of charge density on Ph^1–NH.

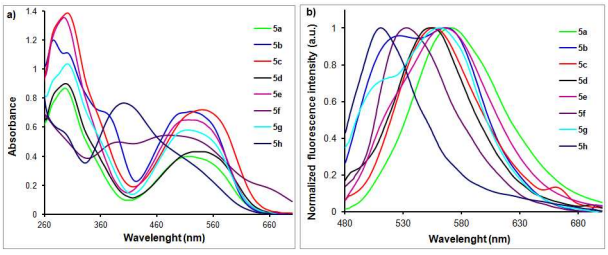

Fig. 5 a) Absorption, b) normalized fluorescence spectra of **5a**–**5h** in DMSO.

Fluorescence quantum yields. The relative fluorescence quantum yields (Φ_x) were calculated by the comparative method (Eq. 1),[50]

$$\Phi_x = \frac{(A_s \times F_x \times n_x^2 \times \Phi_s)}{(A_x \times F_s \times n_s^2)} \qquad \text{Eq. 1}$$

where A is the absorbance at the excitation wavelength, F the area under the fluorescence curve and n the refraction index. Subscripts s and x refer to the standard and the sample of unknown quantum yield, respectively.

The fluorescence quantum yields (Φ_x) of **5a**–**5h** were determined in the DMSO using the Rhodamine 6G (Φ_s = 0.95 in ethanol) as a standard (Table 3).[51] The emission efficiency in dilute solution largely depends on the molecular structure. Compound **5f** provided the highest quantum yield of 0.092, which was unexpected for electron withdrawing NO_2 substituent on the 1-phenyl ring, compared to **5a**–**5e**. Although –Cl and –Br atoms were known to show mesomeric effect, the obtained low quantum yields (Φ_x = 0.041 and 0.043, respectively) rationalized with heavy atom effect. The mesomeric effect of fluorine unit located at the *para*-position of 1-phenyl in compound **5e** was observed with high quantum yield (Φ_x = 0.047), compared to other compound. The lowest quantum yield (Φ_x = 0.038) was observed for the compound **5h** possessing electron-withdrawing nitro-substituents at 2- and 4-positions on the 1-phenyl ring.[52] These Φ_x values indicated that a low number of photons were emitted relative to the number of photons that were deactivated by non-radiative transitions (internal conversion or intersystem crossing), which are favourable if the photons underwent intersystem crossing to the triplet excited state. Based on the outcome of fluorescence investigations, quantum yields are not dependent on the properties of electron–donating and –withdrawing substituents.

Table 3 Absorption and fluorescence characteristics of compounds **5a**–**5h** in DMSO solution.

Compound	Log ε^a	λ_{abs} (nm)^b	λ_{em} (nm)^b	Φ_x^c	S (nm)^d
5a	4.603	513	570	0.045	100
5b	4.732	521	526, 566	0.046	96
5c	4.599	540	556	0.041	86
5d	4.637	533	553	0.043	83
5e	4.665	512	564	0.047	94
5f	4.740	475	532	0.092	62
5g	4.764	513	512, 561	0.046	91
5h	4.885	400	510	0.038	40

[a]Extinction coefficient (1 M^{-1} cm^{-1}). [b]Wavelengths of maximum absorbance (λ_{abs}) and emission intensity (λ_{em}). [c]Φ_x was determined by using Rhodamine 6G in ethanol (Φ = 0.95) as the standard. [d]Stokes shift are calculated as the difference between emission maxima and excitation wavelength (470 nm).

Electrochemical properties

The electrochemical behaviour of the target compounds was probed by cyclic voltammetry in 1 mmol L^{-1} of dichloromethane solution with 0.1 M tetrabutylammonium hexafluorophosphate. The reduction and oxidation curves of **5a**–**5h** are shown in Fig. 6 and the corresponding electrochemical data are summarized in Table 4. Cyclic voltammetry experiments showed the presence of quasi-

reversible oxidation potentials for all the compounds. While the reduction processes were found to be reversible for the compounds **5b**–**5d**, irreversible character for the compounds **5a**, **5e** and **5f** was recorded. Compounds **5g** and **5h** also provided quasi-reversible reduction potential (Fig. 6).

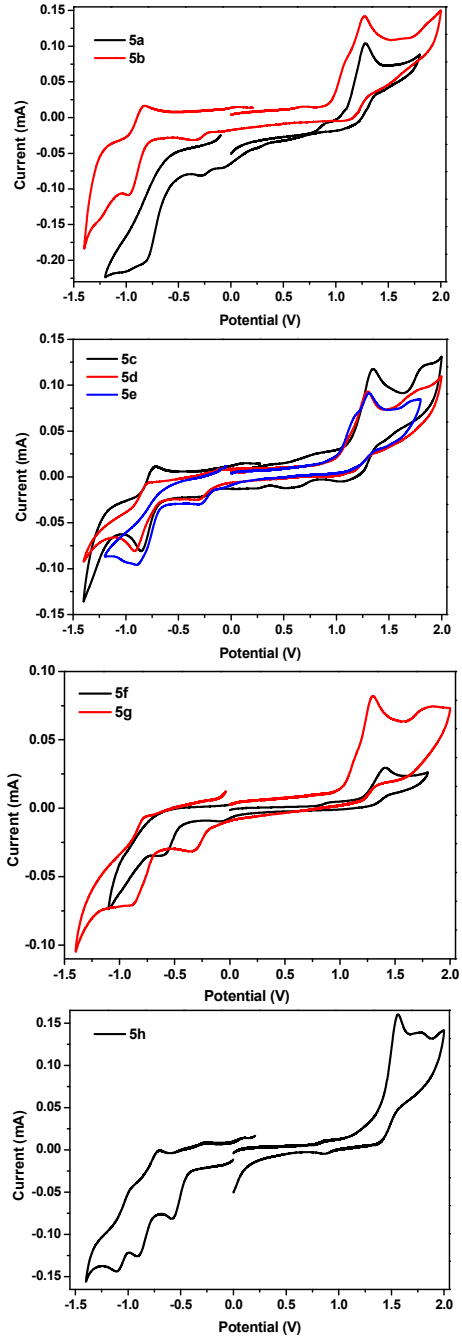

Fig. 6 Cyclic voltammograms of **5a**–**5e** (up) and **5f**–**5h** (down) in 0.1 M Bu_4NPF_6 in dry dichloromethane; run at a sweep rate of 100 mV s^{-1}, showing oxidation and reduction potentials.

Formazans were generally oxidized in two steps and reduced in one step.[17] Formazans **5c**, **5d**, **5g** and **5h** were oxidized by means of the quasi-reversible two-electron transfer process giving the corresponding cation radical. This was followed by the second step in which their tetrazolium cations were formed by giving one e^- and $-H^+$ from the radicals (Scheme 4a).[53] The charge delocalization within systems showing an extended π conjugation further stabilizes the cation radical intermediate.[54] Formazans **5a**, **5b**, **5e** and **5f** were oxidized in a single two-electron process. This electrochemical processes coupled with H^+ transfer giving directly their tetrazolium cations due to a very fast follow-up chemical reaction (Scheme 4b).[27,55,56] The reduction of the tetrazolium cation occurred with a peak potential between of -0.29 to -0.85 V.[17,33] On reducing formazans, probably an anion radical was formed the negative charge on which distributed along all four nitrogen atoms. Formazan structure which consists of four nitrogen atoms and one carbon atom conjugated with three aromatic rings leads to ready electrochemical formation of stable anionic and cationic particles.[53] There is also agreement between these results and the data given in literature.[55-58]

Journal Name RSCPublishing

ARTICLE

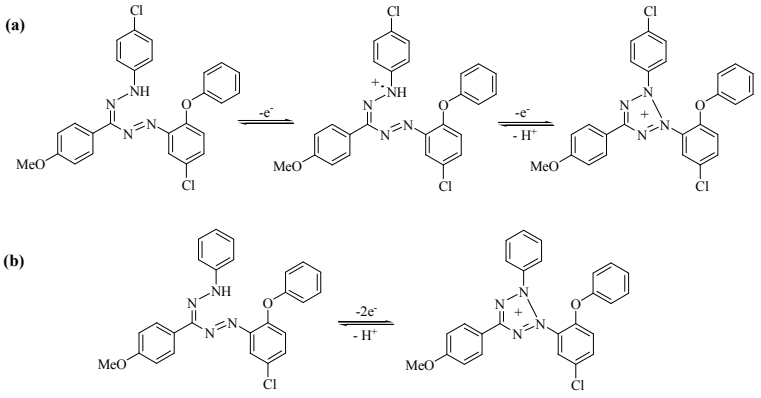

Scheme 4 (a) Schematic representation of structure of **5c** for possible oxidation mechanism of **5c**, **5d**, **5g** and **5h**, (b) structure of **5a** for possible oxidation mechanism of **5a**, **5b**, **5e** and **5f**.

The effect of electron-withdrawing and electron-donating groups at the *N*-aryl substituents was investigated by cyclic voltammetry. The highest first oxidation potential peaks were observed for the compounds **5f** and **5h**, having strong electron withdrawing NO_2 groups. Due to electronegativity of Cl, Br and F atoms, first oxidation potentials were recorded relatively higher for the compounds **5c**, **5d** and **5e**, compared to **5a**. Electron donating groups, such as methoxy and methyl units, reduced the first oxidation potentials. Compound **5b** containing electron-donating –OMe group at *para*-position provided the lowest first oxidation potential, while compound **5h** containing electron withdrawing –NO_2 groups at *ortho*- and *para*-positions has the highest first oxidation potential.

The HOMO−LUMO energy gaps as well as the HOMO and LUMO energies were calculated in order to correlate them with the oxidation and reduction potentials of the investigated **5a**−**5h**. On the basis of the onset potentials, while the HOMO energy levels of **5a**−**5h** were estimated to be between −5.19 and −5.57 eV, the LUMO energy levels were calculated between −3.23 and −4.26 eV, respectively. The cyclic voltammograms of **5a**–**5h** should correlate not with electronic excitation energies but with the electron-acceptor capacity of the substituents, which characterized by the LUMO energies. In addition, electronic band gaps of the new formazans varied between 1.13 and 2.14 eV, respectively (Table 4).

Table 4 Electrochemical properties of the compounds **5a-5h.**

Comp.	E_{ox1} / E_{ox2} (V)[a]	E_{red1} / E_{red2} (V)[a]	E_{ox}^{onset} (V)[b]	E_{red}^{onset} (V)[b]	$E_{HOMO / LUMO}$ (eV)[c]	E_g^{CV} (eV)
5a	1.28	-0.80	1.03	-0.54	-5.43/-3.86	1.58
5b	1.27	-0.35 / -0.97	0.96	-0.21	-5.36/-4.19	1.17
5c	1.34 / 1.83	-0.85	1.13	-0.67	-5.57/-3.73	1.84
5d	1.30 / 1.77	-0.31 / -0.92	0.97	-1.17	-5.37/-3.23	2.14
5e	1.31	-0.29 / -0.88	0.99	-0.14	-5.39/-4.26	1.13
5f	1.41	-0.61	0.79	-0.43	-5.19/-3.97	1.22
5g	1.29 / 1.82	-0.34 / -0.88	1.04	-0.16	-5.44/-4.24	1.20
5h	1.56 / 1.78	-0.58/-0.91/-1.11	1.09	-0.44	-5.49/-3.96	1.53

[a]Oxidation and reduction potentials from cyclic voltammograms. [b]Onsets of oxidation and reduction. [c]HOMO = −(E_{onset} (ox) + 4.4) (eV), LUMO = −(E_{onset} (red) + 4.4).

Theoretical calculations

The geometry optimizations of all synthesized compounds in gas phase were carried out at DFT level of theory using PBE1PBE/6-311g (2d, 2p) level basis set.[59-61] Relative Gibbs free energies and possible tautomeric forms of the each molecule were calculated using the same level of basis set. The results were listed in Tables 5 and 6.

It was believed that the tautomerism of aryl formazans containing at the HN−Ph[1] and N−Ph[5] atoms is an intramolecular process occurring between two degenerate forms.[1,29,34,62,63] According to the calculation results, synthesized formazan derivatives were found in two tautomeric equilibrium due to the proton transfer between the hydrazone nitrogen atom (N4−H1) and the azo group (N2−H2) atoms, which labelled as tautomer 1 and tautomer 2 in formazan frame. Possible tautomeric forms of **5h** were depicted as a representative example in Fig.7.

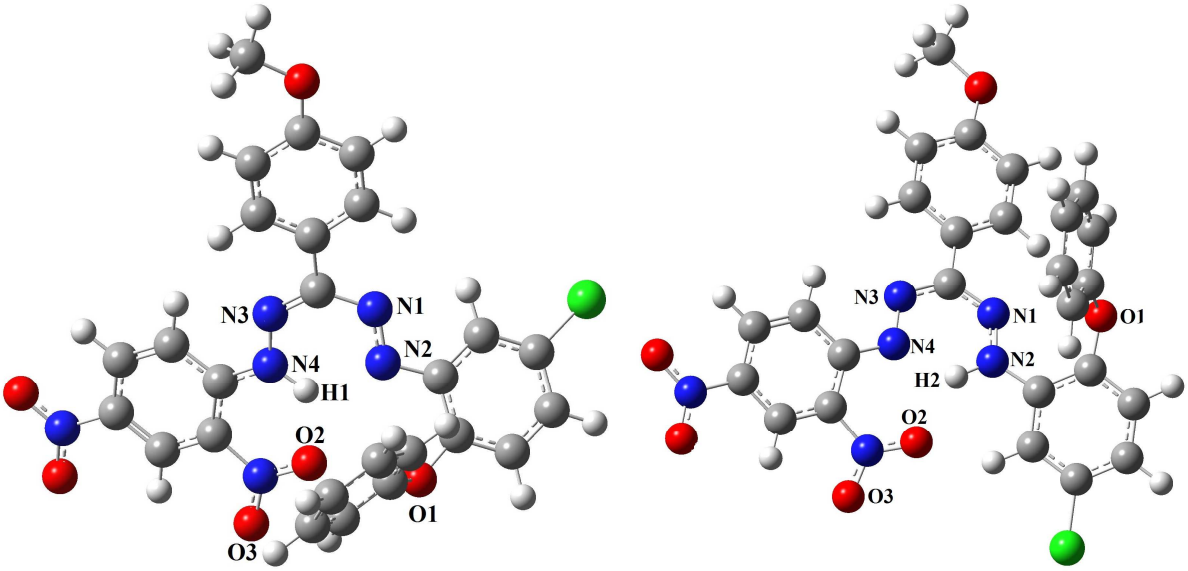

tautomer 1 (**5h**1) tautomer 2 (**5h**2)

Fig. 7 Molecular structures of the possible tautomeric forms of **5h** with atom numbering.

According to the calculation results the stability order of the molecules and the possible tautomeric forms' Gibbs Free Energy based stabilities are as follows **5d**>**5c**>**5h**>**5f**>**5b**>**5e**>**5g**>**5a** (Table 5). These changes observed in the stabilization energy of the molecules may be explained with electronic characteristics of substituent groups in the aromatic ring. This situation can be explained by considering the volume of bromine atom which is greater than that of hydrogen. Therefore the steric effect of bromine was greater than other substituents (−F and −Cl). While electron-withdrawing units increased the stabilization of molecules, electron-donating groups decreased the stabilization energy of molecules.

Table 5 Calculated Gibbs Free Energies (GFE) and selected H–bond values of compounds **5a−5h** and their tautomers by PBE1PBE/6-311G(2d,2p) calculations.

		GFE	H–bond (Å)					
Comp.	Substituents	(Hartree)	H1···N2	H2···N4	H1···O2	H2···O2	H1···O1	H2···O1
5a1	-H	-1371.7337	1.7601		-	-	2.7274	
5a2		-1371.7333		1.8180		-		2.3124
5b1	4-OMe	-1486.1311	1.6314				2.6061	
5b2		-1486.1369		1.8203				2.3108
5c1	4-Cl	-1831.1717	1.6312				2.5801	
5c2		-1831.177		1.8081				2.2984

5d1	4-Br	-3944.8858	1.7522				2.6947	
5d2		-3944.8849		1.8071				2.2981
5e1	4-F	-1470.9251	1.7478				2.7029	
5e2		-1470.9256		1.8142				2.3043
5f1	4-NO_2	-1576.1263	1.7679				2.6797	
5f2		-1576.122		1.7868				2.2852
5g1	3,4-$(CH_3)_2$	-1450.2286			2.7309			
5g2		-1450.2226	1.6825				2.3144	
5h1	2,4-$(NO_2)_2$	-1780.5003		1.9217		3.4258		
5h2		-1780.4909	1.7893		2.1160		3.9855	

In formazans, the equilibrium was fully shifted towards the form where the proton was localised at the nitrogen atom linked to the substituent according to the electronic characteristics.[1] Compounds **5f** and **5h**, which have the strong electron-withdrawing aryl substituents at the Ph–N4 leads to co-existence of tautomer 2 with a considerable amount of the tautomer 1.[1,34] While the molecules **5b**, **5c** and **5e** were stable in tautomer 2 form, molecules **5a**, **5d** and **5g** were also stable tautomer 1 (Table 6). X-ray structural analysis of the compound **5e** determined tautomer 2 as a stable tautomer in solid state. This experimental result has been confirmed by theoretical calculations (Fig. 1 and Fig. 2).

Intramolecular H−bonds (H1···N2, H2···N4, H1···O1, H2···O1, H1···O2 and H2···O2) belonging to possible tautomeric forms of the molecules were investigated (Fig. 7 and Table 5). The difference ΔH were calculated by taking difference between selected H–bonds of the tautomer 1 and 2 (Table 6). H-bonds between H1···N2, which belong to tautomer 1 structure of the molecules **5a**1−**5f**1 was determined to be shorter and stronger H-bonds between H2···N4 beleong to tautomer 2. According to the different hydrogen bonds in molecules **5g**2 and **5h**2, tautomeric form 2 was found to be more stable. When H-bonds between H2···O1 in tautomeric forms 2 of the molecules **5a**−**5g** were compared with H-bonds between H1···O1 in tautomeric form 1, H−bonds between H2···O1 were determined to be shorter and stronger. Likewise tautomeric form 1 appeared to be more stable in the case of molecule **5h**1 owing to the fact that molecule **5h**1 possesses possible H–bonds between oxygen O2 in the *ortho*-NO_2 substituent with H1 and H2. Based on the computations, H bond between H1−O2 was shorter and stronger with respect to the one appearing between H2−O2.

Table 6 Total tautomer stable (ΔK_T) and difference ΔH bond between tautomer forms (**5a**−**5h**).

		ΔH[b]		
Comp.	ΔK_T[a]	A[c]	B[d]	C[e]
5a1 ⇌ **5a**2	0.0004	0.058	-0.415	
5b1 ⇌ **5b**2	-0.0058	0.189	-0.295	
5c1 ⇌ **5c**2	-0.0053	0.177	-0.282	
5d1 ⇌ **5d**2	0.0009	0.055	-0.397	
5e1 ⇌ **5e**2	-0.0005	0.066	-0.399	
5f1 ⇌ **5f**2	0.0043	0.019	-0.395	
5g1 ⇌ **5g**2	0.0059	-0.071	-0.417	
5h1 ⇌ **5h**2	0.0094	-0.227	0.560	0.194

[a] $\Delta K_T = G_{\text{tautomer form 2}} - G_{\text{tautomer form 1}}$, ΔK_T, constant stable between tautomer forms. [b] ΔH, the difference hdyrogen bond between of tautomer forms; [c] A, $\Delta H = \text{H-bond}_{(H2\cdots N4)} - \text{H-bond}_{(H1\cdots N2)}$; [d] B, $\Delta H = \text{H-bond}_{(H2\cdots O1)} - \text{H-bond}_{(H1\cdots O1)}$ [e] C, $\Delta H = \text{H-bond}_{(H2\cdots O2)} - \text{H-bond}_{(H1\cdots O2)}$.

Gibbs free energy and selected H–bonds of the molecules **5a**−**5h** calculated theoretically in gas phase were listed in Table 6. The results of the calculation indicated two different tautomeric forms of the molecules generated by their intramolecular hydrogen bonds in the gas phase.

Conclusions

In this work, a series of novel formazans **5a**–**5h** were synthesized in overall yields of 49–86% which required minimal purification. The structures of the formazans were characterized by using elemental analysis, various spectroscopic methods and the structure of a representative compound **5e** were confirmed based on the X-ray crystallography. UV−Vis measurements indicated that λ_{max} values were somewhat dependent on the solvent polarities. While compounds **5a**–**5d** and **5g**–**5h** showed slight positive solvatochromism, compounds **5e** and **5f** demonstrated negative solvatochromism in polar solvents. The substituent effects were examined in various solvents, which pointed out a bathochromic shift for electron withdrawing units and a hypsochromic shift for electron donating groups. Fluorescence spectral characteristics of the compounds were investigated in DMSO solution. Among all the synthesized derivatives, compound **5a** exhibited yellow fluorescence with the highest emission maximum of 570 nm, whereas compounds **5h** exhibited a green fluorescence with lowest emission maxima of 510 nm. The results showed that emission maximum mainly varied depending on the substituent on 1-phenyl ring. Also the fluorescence quantum yield and Stokes shifts of all compounds were calculated. Electrochemical measurements supported the proposed structures of the target compounds. According to the compuational results the stability order of the molecules and the possible tautomeric forms' Gibbs Free Energy based stabilities are as follows **5d**>**5c**>**5h**>**5f**>**5b**>**5e**>**5g**>**5a**. Spectroscopic explorations and quantum chemical calculations confirmed the existence of a six-membered pseudo aromatic ring hydrogen bond in formazan skeleton and its tautomers due to the inner-molecular hydrogen transfer is consistent with literature. These structural isomers are promising candidates as a ligand for coordination chemistry. Based on these factors, we envision this new class of compounds to be of significant interest in the field of functional materials.

Experimental Section

Materials and instruments

4-Chloro-2-phenoxybenzenamine, substituted phenylhydrazines, 4-methoxybenzaldehyde, NaOH and high grade organic solvents for UV-Vis and fluorescence measurements were purchased from Sigma-Aldrich and used without any further purification. Thin layer chromatography plates (DC-Alufolien Kieselgel 60 F_{254}) were purchased from Merck, Darmstadt. Isolation of compounds was performed by using column chromatography over Sigma Silica gel 60 (63-200 μm).

Microanalyses were carried out using a Leco CHNS-932 elemental analyser. The melting points were measured on a Gallenkamp apparatus using a capillary tube. ^{1}H NMR and ^{13}C NMR spectra were recorded on a Bruker DPX FT-NMR (500 MHz) spectrometer ($SiMe_4$ as internal Standard) and chemical shifts (δ) are given in ppm. The spectrometer was equipped with a 5 mm PABBO BB-inverse gradient probe. The concentration of the solute compounds was 10-15 mg in 1.0 mL of $CDCl_3$ and DMSO-d_6. The FTIR spectra were recorded as KBr pellets using a Bruker IFS 66 v/S FTIR Spectrophotometer in a 4000 - 400 cm^{-1} range at room temperature. The electronic spectra of the formazans (10^{-5} mol L^{-1}) in different solvents were measured using a SHIMADZU UV-3150 UV-VIS-NIR spectrophotometer. The fluorescence spectra of the compounds were recorded on a Cary Eclipse Fluorescence Spectrophotometer (Varian). LC-MS studies of the formazans were carried out with an Agilent 1100 Series LC/MSD Trap VL&SL using atmospheric pressure chemical ionization and electrospray with positive and negative ion detection.

Electrochemical measurements were made using a CH-Instruments Model 400A as a potentiostat. A conventional three-electrode configuration consisting of a platinum working electrode, a Pt-wire counter electrode and an Ag-wire reference electrode was employed. All the measurements were run in dichloromethane with 0.1 M tetrabutylammonium hexafluorophosphate ($[Bu_4N]PF_6$) as the supporting electrolyte at room temperature under nitrogen atmosphere. Ferrocene was added as a calibrant after each set of measurements, and all potentials reported were quoted with reference to the ferrocene/ferrocenium (Fc/Fc^+) couple at a scan rate of 100 mV s^{-1}.

X-ray crystallographic study

Diffraction data for the complex were collected with Bruker AXS APEX CCD diffractometer equipped with a rotation anode at 296(2) K using graphite monochrometed Mo Kα radiation at λ = 0.71073 Å. Diffraction data were collected over the full sphere and were corrected for absorption. The data reduction was performed with the Bruker SMART program package. Structure solution was found with the SHELXS-97 package using the direct methods and was refined SHELXL-97 against F^2 using first isotropic and later anisotropic thermal parameters for all non-hydrogen atoms. Hydrogen atoms were added to the structure model at calculated positions. Geometric calculations were performed with PLATON.

A specimen of $C_{34.67}H_{26.67}Cl_{1.33}F_{1.33}N_{5.33}O_{2.67}$, approximate dimensions of $0.07 \times 0.19 \times 0.76$ mm^3, was used for the X-ray crystallographic analysis. The X-ray intensity data were measured. The integration of the data using an orthorhombic unit cell yielded a total of 105204 reflections to a maximum θ angle of 28.46° (minimum θ angle of 1.50°) (0.75 Å resolution), of which 5570 were independent (average redundancy 18.888, completeness = 99.3%, R_{int} = 14.67%, R_{sig} = 10.85%) and 2799 (50.25%) were greater than 2σ (F^2). The final cell constants of a = 7.8846(3) Å, b = 27.1172(12) Å, c = 20.7714(9) Å, volume = 4441.1(3) Å^3, are based upon the refinement of the XYZ-centroids of reflections above 20σ (I). The calculated minimum and maximum transmission coefficients (based on crystal size) are 0.8547 and 0.9852. The structure was solved and refined using the Bruker SHELXTL Software Package, using the space group P b c a, with Z = 6 for the formula unit, $C_{34.67}H_{26.67}Cl_{1.33}F_{1.33}N_{5.33}O_{2.67}$. The final anisotropic full-matrix least-squares refinement on F^2 with 312 variables converged at R1 = 5.22%, for the observed data and wR2 = 15.06% for all data. The goodness-of-fit was 1.018. The largest peak in the final difference electron density synthesis was 0.469 e$^-$/Å^3 and the largest hole was -0.505 e$^-$/Å^3 with an RMS deviation of 0.170 e$^-$/Å^3. On the basis of the final model, the calculated density was 1.421 g/cm^3 and F (000), 1968 e$^-$.

CCDC 912620 contains the supplementary crystallographic data for compound **5e**. The data can be obtained free of charge via http://www.ccdc.cam.ac.uk/conts/retrieving.html, or from the Cambridge Crystallographic Data Centre, 12 Union Road, Cambridge CB2 1EZ, UK; fax: (+44) 1223-336-033; or e-mail: deposit@ccdc.cam.ac.uk.

Computational method

In the calculations, the CS Chem Office Pro 12.0 for Microsoft Windows[64] and Gaussian09[65] software package with 2 × 6-core Intel Core i7 980X processor, 3.33 GHz, L3 Cache 12 MB, LGA 1366 socket, the X58 chipset workstation was used. Quantum chemical calculations at the DFT Perdew, Burke and Ernzerhof (PBE) functional with basis sets 6-311g (2d, 2p) were done with.[59,60]

Synthesis

Synthesis of substituted phenylhydrazones 3a−3h

The substituted phenylhydrazones **3a**−**3h** were synthesized by condensation of 4-methoxybenzaldehyde with substituted phenylhydrazine compounds (see ESI†).

General Synthesis of formazans 5a−5h

A diazonium salt solution was obtained first. To a solution of 4-chloro-2-phenoxybenzenamine in 10 mL of $HCl_{(aq)}$ (50%, v/v) was dropped a solution of $NaNO_2$ in 5 mL of water at 0–5 °C for 1 h. The reaction mixture was allowed to stir for another 1 h. Completion of diazotization was checked using starch iodide paper. 10 mL of 20% NaOH (1.00 g) was added to a solution of **3a**−**3h** in 20 mL of pyridine at 0 °C. Diazonium salt of 4-chloro-2-phenoxybenzenamine (**4**) was added dropwise with continuous stirring over 1 h, maintaining the temperature below 5 °C. The reaction mixture was allowed to stir for another 3 h and then poured into 250 mL of ice-cold water with continuous stirring. The resulting violet-coloured viscous solid was filtered off, washed with water and recrystallized from methanol.

Preparation of 5-(4-chloro-2-phenoxyphenyl)-3-(4-methoxy-phenyl)-1-phenylformazans (5a). This compound was obtained from **3a** (1.0 g, 4.40 mmol) and diazonium salt **4** (0.96 g, 4.40 mmol). Formazan **5a** (1.65 g, 82%) was obtained as a light violet powder with a melting point of 176−177 °C. R_f : 0.63 (*n*-hexane/ethyl acetate, 5:1). Anal. Calcd. for $C_{26}H_{21}ClN_4O_2$ (%) : C, 68.34; H, 4.63; N, 12.26; found : C, 68.12; H, 4.75; N, 11.97. FT-IR (KBr, cm^{-1}) ν_{max} : 3055(w),, 1361 (s), 1587 (s), 3010 (s), 1596 (s), 1492 (s), 1249-1211 (m). ^{1}H NMR (500 MHz, $CDCl_3$): δ 15.23 (s, 1H), 8.12 (d, *J* = 8.73 Hz, 2H), 8.04 (d, *J* = 2.39 Hz, 1H), 7.67 (t, *J* = 7.57 Hz, 2H), 7.43 (d, *J* = 7.73 Hz, 2H), 7.40 (m, 3H), 7.19 (t, *J* = 7.42 Hz, 1H), 7.13 (d, *J* = 8.40 Hz, 2H), 7.03 (d, *J* = 8.73 Hz, 2H), 6.98 (dd, *J* = 8.54 and 2.45 Hz, 1H), 6.87 (d, *J* = 8.61 Hz, 1H), 3.90 (s, 3H). ^{13}C NMR (126 MHz, $CDCl_3$): δ 159.75, 156.66, 151.36, 143.63, 142.49, 137.44, 130.64, 130.30, 130.09, 129.84, 129.21, 127.53, 123.89, 123.53, 121.73, 119.83, 118.18, 114.89, 113.88, 55.39. ESI-MS *m/z* : 457.1 ($(M + H)^+$, 18%); 456.1 ($(M)^+$, 13%); 455.1 ($(M - H)^+$, 50%). ESI-MS/MS *m/z* : 318.2 (100 %); 304.3 (87 %); 244.3 (6 %).

5-(4-Chloro-2-phenoxyphenyl)-1,3-bis(4-methoxyphenyl)-formazan (5b). This compound was obtained from **3b** (1.50 g, 5.90 mmol) and diazonium salt **4** (1.29 g, 5.90 mmol) as a red solid. Anal. Calcd. for $C_{27}H_{23}ClN_4O_3$ (%) : C, 66.60; H, 4.76; N, 11.51; found : C, 66.85; H, 4.89; N, 11.24. Yield: 1.68 g (59 %); R_f : 0.48 (*n*-hexane/ethyl acetate, 5:1); m.p. 164−166 °C; FT-IR (KBr, cm^{-1}) ν_{max} : 3068 (w), 1352 (s), 1583 (s), 3004 (s), 1596 (s), 1461 (s), 1253-1215 (m). ^{1}H NMR (500 MHz, $CDCl_3$): *δ* 14.87 (s, 1H), 8.10 (d, *J* = 8.56 Hz, 2H), 8.00 (d, *J* = 2.03 Hz, 1H), 7.69 (d, *J* = 8.64 Hz, 2H), 7.42 (t, *J* = 7.65 Hz, 2H), 7.18 (t, *J* = 7.33 Hz, 1H), 7.12 (d,

J = 8.35 Hz, 2H), 7.02 (d, *J* = 8.55 Hz, 2H), 6.91 (d, *J* = 8.45 Hz, 3H), 6.83 (d, *J* = 8.56 Hz, 1H), 3.88 (s, 6H). ^{13}C NMR (126 MHz, $CDCl_3$): δ 162.54, 159.70, 156.78, 146.65, 142.42, 142.37, 137.02, 130.35, 130.26, 130.05, 129.94, 129.48, 128.81, 127.67, 126.51, 124.31, 123.75, 122.00, 119.72, 118.07, 114.53, 114.43, 114.09, 113.98, 55.65, 55.38 (2C). ESI-MS *m/z :* 487.1 ($(M + H)^+$, 34%); 486.1 ($(M)^+$, 28%); 485.1 ($(M – H)^+$, 100%). ESI-MS/MS *m/z* : 350.0 (4%); 230.9 (5 %); 168.0 (32%).

5-(4-Chloro-2-phenoxyphenyl)-3-(4-methoxyphenyl)-1-(4-chlorophenyl)formazan (5c). This compound was obtained from **3c** (1.20 g, 4.60 mmol) and diazonium salt **4** (1.01 g, 4.60 mmol) as a claret solid. Anal. Calcd. for $C_{26}H_{20}C_{l2}N_4O_2$ (%) : C, 63.55; H, 4.10; N, 11.40; found : C, 63.36; H, 4.25; N, 11.18. Yield: 1.64 g (73%); R_f : 0.80 (*n*-hexane/ethyl acetate, 5:1); m.p. 164−166 ^{o}C; FT-IR (KBr, cm^{-1}) ν_{max} : 3074 (w), 1353 (s), 1587 (s), 3010 (s), 1598 (s), 1490 (m), 1249-1215 (m). ^{1}H NMR (500 MHz, $CDCl_3$): δ 15.20 (s, 1H), 8.07 (d, *J* = 8.81 Hz, 2H), 8.03 (d, *J* = 2.31 Hz, 1H), 7.49 (d, *J* = 7.57 Hz, 2H), 7.47 (d, *J* = 8.82 Hz, 2H), 7.43 (t, *J* = 7.93 Hz, 2H), 7.21 (t, *J* = 7.37 Hz, 1H), 7.11 (d, *J* = 7.83 Hz, 2H), 7.04 (d, *J* = 8.79 Hz, 2H), 7.03 (d, *J* = 8.45 Hz, 1H), 6.87 (d, *J* = 8.62 Hz, 1H), 3.81 (s, 3H). ^{13}C NMR (126 MHz, $CDCl_3$): δ 159.81, 156.54, 149.98, 143.94, 142.64, 137.36, 132.42, 130.36, 130.17, 129.61, 127.47, 124.49, 124.11, 124.04, 122.85, 119.85, 118.15, 114.98, 113.90, 55.38. ESI-MS *m/z :* 491.0 ($(M + H)^-$, 70%); 490.0 ($(M)^-$, 70%); 489.0 ($(M – H)^-$, 35%). ESI-MS/MS *m/z* : 395.9 (20%); 284.9 (7%); 250.8 (21%); 202.8 (100%); 174.9 (22%).

5-(4-Chloro-2-phenoxyphenyl)-3-(4-methoxyphenyl)-1-(4-bromophenyl)formazan (5d). This compound was obtained from **3d** (1.20 g, 3.90 mmol) and diazonium salt **4** (0.86 g, 3.90 mmol) as a dark violet solid. Anal. Calcd. for $C_{26}H_{20}BrClN_4O_2$ (%) : C, 58.28; H, 3.76; N, 10.46; found : C, 58.15; H, 3.84; N, 10.43. Yield: 1.81 g (86%); R_f : 0.75 (*n*-hexane/ethylacetate, 5:1); m.p. 177−178 ^{o}C; FT-IR (KBr, cm^{-1}) ν_{max} : 3066 (w), 1352 (s), 1587 (s), 3012 (s), 1598 (s), 1490 (m), 1247-1215 (m). ^{1}H NMR (500 MHz, $CDCl_3$): δ 15.25 (s, 1H), 8.07 (d, *J* = 8.78 Hz, 2H), 8.02 (d, *J* = 2.26 Hz, 1H), 7.55 (d, *J* = 8.65 Hz, 2H), 7.42 (t, *J* = 7.92 Hz, 2H), 7.34 (d, *J* = 8.68 Hz, 2H), 7.20 (t, *J* = 7.39 Hz, 1H), 7.10 (d, *J* = 8.00 Hz, 2H), 7.01 (d, *J* = 8.76 Hz, 2H), 6.98 (d, *J* = 2.23 Hz, 1H), 6.86 (d, *J* = 8.65 Hz, 1H), 3.89 (s, 3H). ^{13}C NMR (126 MHz, $CDCl_3$): δ 159.80, 156.56, 149.78, 143.71, 142.60, 137.23, 136.29, 130.36, 130.16, 129.63, 129.45, 127.48, 124.02, 123.88, 122.76, 119.83, 118.13, 114.95, 113.90, 55.38. ESI-MS *m/z* : 536.1 ($(M + 2H)^-$, 28%); 535.1 ($(M + H)^-$, 23%); 534.0 ($(M)^-$, 100%). ESI-MS/MS *m/z* : 294.8 (19%); 255.1 (18%); 202.8 (100%).

5-(4-Chloro-2-phenoxyphenyl)-3-(4-methoxyphenyl)-1-(4-fluorophenyl)formazan (5e). This compound was obtained from **3e** (1.20 g, 3.90 mmol) and diazonium salt **4** (0.86 g, 4.90 mmol) as a red solid. Anal. Calcd. for $C_{26}H_{20}ClFN_4O_2$ (%) : C, 65.75; H, 4.24; N, 11.80; found : C, 65.45; H, 4.33; N, 11.83. Yield : 2.18 g (70%); R_f : 0.71 (*n*-hexane/ethyl acetate, 5:1); m.p. 158−160 ^{o}C; FT-IR (KBr, cm^{-1}) ν_{max} : 3068 (w), 1359 (s), 1508 (s), 3005 (s), 1589 (s), 1494 (m), 1245-1211 (m). ^{1}H NMR (500 MHz, $CDCl_3$): δ 15.09 (s, 1H), 8.08 (d, *J* = 8.83 Hz, 2H), 8.01 (d, *J* = 2.40 Hz, 1H), 7.66 (dd, *J* = 8.84, 5.25 Hz, 2H), 7.43 (t, *J* = 7.96 Hz, 2H), 7.19 (t, *J* = 7.40 Hz, 1H), 7.10 (d, *J* = 7.64 Hz, 2H), 7.07 (d, *J* = 8.44 Hz, 2H), 7.01 (d, *J* = 8.84 Hz, 2H), 6.95 (dd, *J* = 8.60 and 2.42 Hz, 1H), 6.84 (d, *J* = 8.59 Hz, 1H), 3.92 (s, 3H). ^{13}C NMR (126 MHz, $CDCl_3$): δ 165.37, 163.36, 159.78, 156.63, 148.49, 148.47, 142.92, 142.41, 136.88, 130.38, 130.12, 129.67, 127.52, 124.04, 123.97, 123.93, 123.01, 119.77, 118.07, 116.34, 116.15,114.80, 113.87, 55.37. ESI-MS *m/z* : 475.0 ($(M + H)^-$, 34%); 474.0 ($(M)^-$, 28%); 473.1 ($(M – H)^-$, 100%). ESI-MS/MS *m/z* : 268.9 (47%); 234.8 (28%); 202.8 (100%).

5-(4-Chloro-2-phenoxyphenyl)-3-(4-methoxyphenyl)-1-(4-nitrophenyl)formazan (5f). This compound was obtained from **3f** (1.50 g, 5.50 mmol) and diazonium salt **4** (1.22 g, 5.50 mmol) as a darkish solid. Anal. Calcd. for $C_{26}H_{20}ClN_5O_4$ (%) : C, 62.22; H, 4.02; N, 13.95; found : C, 61.95; H, 4.09; N, 13.92. Yield : 1.60 g (58%); R_f : 0.86 (*n*-hexane/ethyl acetate, 5:1); m.p. 211-213 ^{o}C; FT-IR (KBr, cm^{-1}) ν_{max} : 3076 (w), 1371 (s), 1502 (s), 3004 (s), 1591 (s), 1471 (m), 1249-1213 (m). ^{1}H NMR (500 MHz, $CDCl_3$): δ 15.38 (s, 1H), 8.15 (d, 2H), 8.09 (d, 2H), 7.99 (s, 1H), 7.46 (d, 2H), 7.34 (s, 1H), 7.26 (s, 1H), 7.23 (m, 3H), 7.16 (d, 2H), 7.00 (s, 2H), 3.82 (s, 3H). ^{13}C NMR (126 MHz, $CDCl_3$): δ 160.23, 156.25, 151.81, 150.19, 143.70, 143.43, 141.96, 131.70, 130.53, 130.11, 129.07, 127.71, 126.21, 125.54, 124.76, 120.51, 118.88, 115.99, 115.48, 114.06, 55.42. ESI-MS *m/z* : 502.0 ($(M + H)^+$, 35%); 501.1 ($(M)^+$, 28%); 500.1 ($(M – H)^+$, 100%). ESI-MS/MS *m/z* : 350.0 (15%); 230.9 (20%); 168.0 (100%).

5-(4-Chloro-2-phenoxyphenyl)-3-(4-methoxyphenyl)-1-(3,4-dimethylphenyl)formazan (5g). This compound was obtained from

3g (1.50 g, 5.90 mmol) and diazonium salt **4** (1.30 g, 5.90 mmol) as a red solid. Anal. Calcd. for $C_{28}H_{25}ClN_4O_2$ (%) : C, 69.34; H, 5.20; N, 11.55; found : C, 69.11; H, 5.28; N, 11.27. Yield : 1.78 g (62%); R_f : 0.70 (*n*-hexane/ethyl acetate, 5:1); m.p. 173−175 ^oC; FT-IR (KBr, cm^{-1}) ν_{max} : 3074 (w), 1363 (s), 1587 (s), 3041 (s), 1598 (s), 1490 (m), 1249-1217 (m). ^1H NMR (500 MHz, $CDCl_3$): δ 15.27 (s, 1H), 8.12 (d, J = 8.03 Hz, 2H), 8.02 (s, 1H), 7.48 (s, 1H), 7.43 (t, J = 7.51 Hz, 2H), 7.20 (d, J = 7.34 Hz, 2H), 7.16 (d, J = 8.20 Hz, 3H), 7.02 (d, J = 8.13 Hz, 2H), 6.93 (d, J = 8.60 Hz, 1H), 6.85 (d, J = 8.55 Hz, 1H), 3.90 (s, 3H), 2.20-2.30 (s, 6H). ^{13}C NMR (126 MHz, $CDCl_3$): δ 159.69, 156.71, 150.30, 142.98, 142.40, 140.71, 137.60, 137.14, 130.42, 130.22, 130.06, 130.02, 127.57, 124.45, 123.83, 122.53, 119.50, 118.55, 118.28, 114.59, 113.83, 55.37, 19.92, 19.67 (2C). ESI-MS *m/z* : 485.1 ($(M + H)^-$, 41%); 484.1 ($(M)^-$, 30%); 483.1 ($(M – H)^-$, 100%). ESI-MS/MS *m/z* : 377.0 (6%); 270.8 (4%); 216.8 (34%); 202.8 (100%).

5-(4-Chloro-2-phenoxyphenyl)-3-(4-methoxyphenyl)-1-(2,4-dinitrophenyl)formazan (5h). This compound was obtained from **3h** (1.50 g, 4.70 mmol) and diazonium salt **4** (1.04 g, 4.70 mmol) as a brown solid. Anal. Calcd. for $C_{26}H_{19}ClN_6O_6$ (%) : C, 57.10; H, 3.50; N, 15.37; found : C, 56.83; H, 3.75; N, 15.29. Yield : 1.26 g (49%); R_f : 0.68 (*n*-hexane/ethyl acetate, 5:1); m.p. 192−193 ^oC; FT-IR (KBr, cm^{-1}) ν_{max} : 3093 (w), 1332 (s), 1591 (s), 3014 (s), 1610 (s), 1496 (m), 1253-1207 (m). ^1H NMR (500 MHz, $CDCl_3$): δ 13.95 (s, 1H), 9.25 (s, 1H), 8.88 (s, 2H), 8.38 (s, 2H), 8.01 (s, 1H), 7.85 (m, 2H), 7.43 (m, 1H), 7.15 (m, 4H), 7.10 (m, 2H), 3.85 (s, 3H). ^{13}C NMR (126 MHz, $CDCl_3$): δ 161.16, 156.76, 154.92, 149.92, 145.57, 144.47, 144.08, 141.25, 139.27, 134.49, 130.07, 129.96, 127.15, 124.87, 124.27, 123.27, 121.19, 119.26, 117.20, 113.94, 55.42. ESI-MS *m/z* : 545.0 ($(M – H)^+$, 28%); 546.1 ($(M)^+$, 100%). ESI-MS/MS *m/z* : 485.1 (100%); 391.9 (27%); 167.9 (41%).

Acknowledgements

We are very grateful to the Anadolu University Research Fund for providing financial support for this project (Projects No : 1004F94 and 1102F027). We are grateful to the Medicinal Plants and the Medicine Research Center of Anadolu University Eskişehir (Turkey) for the NMR and X-ray measurements.

Notes and references

[a] Anadolu University, Faculty of Science, Chemistry Department, 26470 Eskişehir, Turkey

†Electronic Supplementary Information (ESI) available: [Experimental procedures and characterization data of compounds (**3a**-**3h**), crystallographic data, absorption spectra data and NMR spectra of final compounds (**5a**−**5h**)]. See DOI: 10.1039/b000000x/

1 G. I. Sigeikin, G. N. Lipunova and I. G. Pervova, *Russ. Chem. Rev.,* 2006, **75**, 885.
2 H. Y. Zhang, W. X. Sun, Q. A. Wu, H. Q. Zhang, Y. Y. Chen, *Synth. React. Inorg. Met.,* 2000, **30**, 571.
3 A.V. Zaidman, I. G. Pervova, A. I. Vilms, G. P. Belov, R. R. Kayumov, P. A. Slepukhin and I. N. Lipunov, *Inorg. Chim. Acta,* 2011, **367**, 29.
4 J. P. Raval, P. R. Patel, N. H. Patel, P. S. Patel, V. D. Bhatt and K. N. Patel, *Int. J. Chem. Tech. Res.,* 2009, **1**(3), 610.
5 H. Tezcan, *Spectrochim Acta A,* 2008, **69**, 971.
6 L. S. Atabekyan, V. A. Barachevskii, S. A. Melkozerov, G. N. Lipunova, I. G. Pervova, I. N. Lipunov and G. I. Sigeikin, *High Energ. Chem.,* 2011, **45**, 52.
7 I. G. Pervova, V. A. Barachevskii, S. A. Melkozerov, G. N. Lipunova, G. I. Sigeikin and I. N. Lipunov, *Photochemistry,* 2010, **44**, 20.
8 A. R. Katritzky, S. A. Belyakov, D. Cheng and H. D. Durst, *Synthesis*, 1995, **5**, 577.
9 V. Zsoldos-Mády, I. Pintér, P. Sándor, M. Peredy-Kajtár and A. Messmer, *J. Carbohyd. Chem.,* 2001, **20**, 747.
10 Y. A. Ibrahim, A. A Abbas and A. H. M. Elwahy, *J. Heterocyclic Chem.,* 2004, **41**, 135.
11 R. R. Nadendla and A. N. Babu, *J. Pharm. Res.* 2011, **4**, 3.
12 J. P. Raval, T. N. Akhaja, H. V. Patel, N. H. Patel and S. Patel, *Int. J. Pharm. Res.,* 2009, **1**, 62.
13 A. B. Samel and N. R. Pai, *J. Chem. Pharm. Res.,* 2010, **2**, 60.
14 S. I. Marjadi, J. H. Solanki and A. L. Patel, *E-J. Chem.,* 2009, **6**, 844.
15 J. P. Raval, P. Patel and P. S. Patel, *Int. J. Pharm. Tech. Res.,* 2009, **1**, 1548.
16 G. N. Lipunova, Z. G. Rezinskikh, T. I. Maslakova, P. A. Slepukhin, I. G. Pervova, I. N. Lipunov and G. I. Sigeikin, *Russ. J. Coord. Chem.,* 2009, **35**, 215.
17 N. A. Frolova, S. Z. Vatsadze, A. I. Stasha, R. D. Rakhimov and N. V. Zyk, *Chem. Heterocycl. Com.,* 2006, **42**, 1444.
18 A. Iqbal, M. G. Moloney, H. L. Siddiqui and A. L. Thompson, *Tetrahedron Lett.,* 2009, **50**, 4523.
19 I. G. Pervova, P. A. Slepukhin, A. V. Zaidman, G. N. Lipunova and I. N. Lipunov, *Russ. J. Coord. Chem.,* 2010, **36**, 213.
20 M. C. Chang, T. Dann, D. P. Day, M. Lutz, G. G. Wildgoose and E. Otten, *Angew. Chem.,* 2014, **126**, 1; *Angew. Chem. Int. Ed.,* 2014, **53**, 4118.
21 J. B. Gilroy, M. J. Ferguson, R. McDonald, B. O. Patrickc and R. G. Hicks, *Chem. Commun.,* 2007, 126.
22 M.-C. Chang and E. Otten, *Chem. Commun.,* 2014, **50**,7431.

23 S. M. Barbon, P. A. Reinkeluers, J. T. Price, V. N. Staroverov and J. B. Gilroy, *Chem. Eur. J.,* 2014, **20**, 11340.
24 S. H. Moussa, A. A. Tayel, A. A. Al-Hassan and A. Farouk, *Hindawi Publishing Corporation Journal of Mycology*, 2013, **ID753692**, 1.
25 D. M. Aziz, *Anim. Reprod. Sci.,* 2006, **92**, 1.
26 D. Creanga and C. Nadejde, *Chemical Papers*, 2014, **68**, 260.
27 H. Tezcan, E. Uzluk and M. L. Aksu, *J. Elect. Chem.,* 2008, **619–620**, 105.
28 R. A. King and B. Murrin, *J. Phys. Chem. A*, 2004, **108**, 4961.
29 H. Tavakol, *Int. J. Quantum Chem.,* 2012, **112**, 1215.
30 K. Ali, H. A. Eyada, M. T. Abd El-Rahman, M. H. Helal, M. S. Abd-Elal.El-Gaby and G.-H. Ali, *J. Mater. Sci. Eng. B,* 2011, **1**, 461.
31 M. P. Divya, G. B. Mahajan, V. P. Kamat, C. G. Naik, R. R. Parab and N. R. Thakur, *Mar. Drugs,* 2009, **7**, 464.
32 S. G. Kini, A. Bhat, Z. Pan and FE. Dayan, *J. Enzyme Inhib. Med. Chem*. 2010, **25**, 730.
33 H. Gorcay, G. Turkoglu, Y. Sahin and H. Berber, *IEEE Sensors Journal,* 2014, **14**, 2529-36.
34 A. W. Nineham, *Chem. Rev.,* 1955, **55**, 355.
35 V. M. Dziomko, V. M. Ostrovskaya and T. E. Zhukova, *Khim. Geterotsikl. Soedin.,* 1979, **8**, 1039.
36 O. E. Sherif, *Monatsh. Chem.,* 1997, **128**, 981.
37 G. Arnold and C. Schiele, *Spectrochim. Acta A,* 1969, **25A**, 685.
38 A. P. Zeif, N. N. Shchegoleva, G. N. Lipunova, A. P. Novikova and N. V. Bednyagina, *Zhur. Org. Khim.,* 1970, **6**, 1332.
39 A. A. Abbas and A. H. M. Elwaby, *Arkivoc*, 2009, **(x)**, 65.
40 G. Mariappan, R. Korim, N. M. Joshi, F. Alam, R. Hazarika, D. Kumar and T. Uriah, *J. Adv. Pharm. Tech. Res.,* 2010, **1**, 396.
41 Y. A. Ibrahim, *Tetrahedron,* 1997, **53**, 8507.
42 H. Tezcan, S. Can and R. Tezcan, *Dyes and Pigments,* 2002, **52**, 121.
43 Y. A. Ibrahim, A. A. Abbas and A. H. M. Elwaby, *J. Heterocycl. Chem.,* 2004, **41**, 135.
44 A. P. Zeif, G. N. Lipunova, N. P. Bednyagina, L. N. Shchegoleva and L. I. Chernyavskii, *Zh. Org. Khim.,* 1970, **6**, 2590.
45 H. Tezcan and N. Ozkan, *Dyes Pigments,* 2003, **56**, 159.
46 H. Tezcan and E. Uzluk, *Dyes and Pigments*, 2007, **75**, 633.
47 M. Homocianu, A. Airinei and D. O. Dorohoi, *J. Adv. Res. Phys.,* 2011, **2**, 1.
48 A. Sharma and S. G. Schulman, Introduction to fluorescence spectroscopy, John Wiley & Sons, New York, 1999.
49 J. R. Lakowicz, Principles of fluorescence spectroscopy, Springer, New York, 2003.
50 S. R. Meech and D. Phillips, *J. Photo. Chem.,* 1983, **23**, 193.
51 R. F. Kubin and A. N. Fletcher, *J. Luminescence,* 1982, **27**, 455.
52 M. El-Sedik, N. Almonasy, M. Nepras, F. Bures, M. Dvorák, M. Michl, J. Cermák and R. Hrdina, *Dyes and Pigments,* 2012, **92**, 1126.
53 M. Lacan, I. Tabakovic and Z. Cekovic, *Tetrahedron,* 1974, **30**, 2911.
54 R. Y. Lai, K. Xiangxing, S. A. Jenekhe and AJ. Bard, *J. Am. Chem. Soc.,* 2003, **125**, 12631.
55 G. M. Abou-Elenien, *J. Elect. Chem.,* 1994, **375**, 301.
56 H. Tezcan and G. Ekmekci, *Acta Chim. Slov.,* 2010, **57**, 189.
57 T. Oritani, N. Fukuhara, T. Okajima, F. Kitamura and T. Ohsaka, *Inorg. Chim. Acta,* 2004, **357**, 436.
58 H. Tezcan, H. Senoz and N. Tokay, *Monatsh. Chem.,* 2012, **143**, 579.
59 J. P. Perdew, K. Burke and M. Ernzerhof, *Phys. Rev. Lett.,* 1996, **77**, 3865.
60 H. Tezcan and N. Tokay, *Spectrochimica Acta Part A,* 2010, **75**, 54.
61 H. Tezcan and N. Tokay, *Int. J. Quantum Chem.,* 2010, **110**, 2140.
62 H. Senoz, *Hacet. J. Biol. Chem.,* 2012, **40**, 293.
63 M. Toy, H. Tanak and H. Senoz, *Dyes and Pigments*, 2015, **113**, 510.
64 CS ChemBioDraw Ultra 12.0 Download Individual One Year Term English Windows. 2010.
65 Gaussian 09. Revision B.01. M. J. Frisch, G. W. Trucks, H. B. Schlegel, G. E. Scuseria, M. A. Robb, J. R. Cheeseman, G. Scalmani, V. Barone, B. Mennucci, G. A. Petersson, H. Nakatsuji, M. Caricato, X. Li, H. P. Hratchian, A. F. Izmaylov, J. Bloino, G. Zheng, J. L. Sonnenberg, M. Hada, M. Ehara, K. Toyota, R. Fukuda, J. Hasegawa, M. Ishida, T. Nakajima, Y. Honda, O. Kitao, H. Nakai, T. Vreven, J. A. Jr. Montgomery, J. E. Peralta, F. Ogliaro, M. Bearpark, J. J. Heyd, E. Brothers, K. N. Kudin, V. N. Staroverov, R. Kobayashi, J. Normand, K. Raghavachari, A. Rendell, J. C. Burant, S. S. Iyengar, J. Tomasi, M. Cossi, N. Rega, N. J. Millam, M. Klene, J. E. Knox, J. B. Cross, V. Bakken, C. Adamo, J. Jaramillo, R. Gomperts, R. E. Stratmann, O. Yazyev, A. J. Austin, R. Cammi, C. Pomelli, J. W. Ochterski, R. L. Martin, K. Morokuma, V. G. Zakrzewski, G. A. Voth, P. Salvador, J. J. Dannenberg, S. Dapprich, A. D. Daniels, Ö. Farkas, J. B. Foresman, J. V. Ortiz, J. Cioslowski and D. J. Fox, Gaussian Inc Wallingford CT, 2009.

